regard to the characterization of HTV, injury mechanism, tool designs, and dose-response relationships.

Theoretical modeling of the hand-arm system to study its biodynamic response has been traditionally conducted using mechanical models, composed of lumped mass, spring and damper elements.(Dong et al. 2001) These types of models, however, cannot represent a static/dynamic deformation behavior of a local region in the hand-arm system. With a recent progress in computer CPU power, in contrast, other theoretical models, analytical and finite element (FE) models, that describe the mechanical properties of local structures of the living soft tissue, have been developed to simulate the biodynamic responses between hand-arms and tool grips and to predict these mechanical stimuli the soft tissue in palms receives during operation of hand power tools. (Dong et al. 2005)

A two-dimensional FE fingertip model, composed of soft tissue, bone, and nail, has been proposed to simulate the stress-strain distributions in the fingertip indented by rectangular gratings.(Srinivasan and Dandekar 1996) Another two-dimensional FE model of the finger pad has been proposed but no empirical verifications on the capabilities of the model were performed. (Maeno et al. 1998) A three-dimensional FE fingertip model has been developed in which the responses of the slowly adapting type I (SA-I) mechanoreceptors to indentations by complex object shapes was examined. (Dandekar et al. 2003) These FE models regarded the soft tissues as linearly elastic and inviscid. In contrast, nonlinear two-dimensional FE fingertip models have been proposed at the beginning of 2000s. (Wu et al. 2002a; Wu et al. 2002b) In these models, the soft tissue regions were modeled based on the biphasic theory (Mow et al. 1980), which describes the viscoelastic property of the soft tissue during deformation as the interaction between the solid and fluid phase of the tissue. However all the models have not taken account of environmental conditions that affect the vibrotactile threshold in fingertips.

Our final goal in this study is to construct a computational hand-arm system that can predict the dynamic responses of the hand-arm system exposed to HTV under arbitrary environmental conditions characterized by environmental temperature, humidity, surface temperature of tool grips, perspiration in palms, and so on. The successful construction of this computational hand-arm system enables us to predict TTS in hand-transmitted vibration induced by various environmental factors. This study proposes a novel biodynamic response model based on FEM that combines the heat transfer equation with the momentum equation. This combination includes modeling of decrease in skin temperature in hand-arms exposed to HTV and that of the tissue mechanical properties as a function of thermal environment and humidity. As the first report of this study, this paper presents the general concept of fabrication of a finite element model for the computational hand-arm system that couples the heat transfer equation in bio-tissues with the wave propagation equation.

2. Materials and Methods

2.1 Neurophysiologic modeling

Figure 1 schematically shows the structure of the skin tissue and the positions and sizes of the mechanoreceptors in the skin tissue. The skin tissue mainly consists of epidermis, dermis, and subctis. The papillae are the folds at the interface between the dermis and epidermis. Mechanoreceptors hat respond to the mechanical pressure or distortion are found in the skin tissue of fingertips and palms. As summarized in Table 1, the mechanoreceptors are classified into four main types: Pacinian corpuscles, Meissner's corpuscles, Merkel's discs, and Ruffini endings. Among the four types, Pacinian corpuscles and Meissner's corpuscles detects vibrations. Pacinian corpuscles, with a length ranging from 0.5 to 2 mm, and a diameter of about 0.7 mm, are located in the middle of the reticular dermis, which detects vibrations of relatively high vibratory frequency ranging from 40 to 400 Hz. In contrast, Meissner's corpuscle, with a size of about 150 μ m and a diameter ranging from 40 to 70 μ m, are located at the tip of the papillary dermis, which detects vibrations of comparatively low vibratory frequency ranging from 5 to 60 Hz. In our finite element model, some nodes corresponding to the anatomical position for the mechanoreceptors were allocated to these mechanoreceptors.

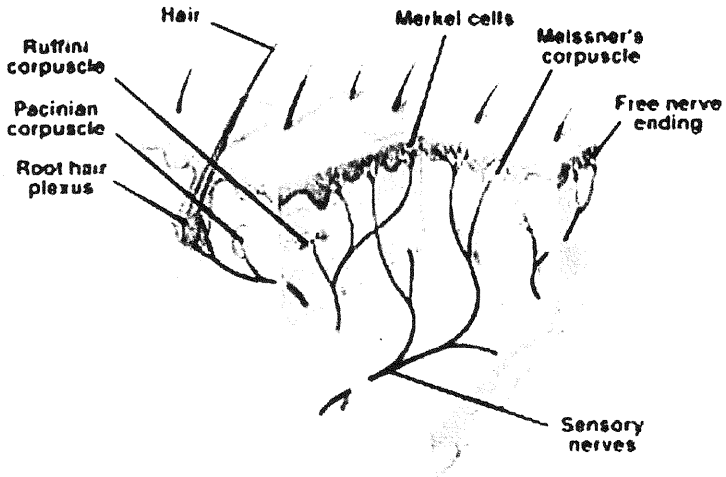

Fig. 1 Schematic view of cross-section of the upper part of the human skin tissue (Gray and Clemente 1985)

Table 1 Characteristics of mechanoreceptors(Mansfield 2004).

Receptor name	Adaptation	Receptive fields	Frequency range (Hz)
Meissner's corpuscle	Rapid	Small	5-60
Pacinian corpuscle	Rapid	Large	40-400
Merkel's disc	Slow	Small	0-5
Ruffini ending	Slow	Large	100-500 (pressure/stretching)

2.2 Finite element modeling

As a fundamental step on the fabrication of the FE model for biodynamic response simulation, a two-dimensional cross-sectional FE model is proposed. Figure 2 shows the schematic illustration of the cross section of the human index finger. The finger consists of three layers of epidermis, dermis, and subctis (including tendons), the core of which is finger bone. Four arteries lie in a direction perpendicular to the paper, around the finger bone in the subctis. The two-dimensional model neglects the blood flow of the arteries suggesting that the temperature and the flow rate of the artery blood are invariant.

Another cross-section model can be considered in the sagittal plane of fingers. We plan to consider the dynamics of blood flow in arteries to take a function of heat exchanger into account. As shown in Fig. 3, our final target is to construct step by step the 3-D computational entire hand-arm system that of course includes the upper and lower arms, too.

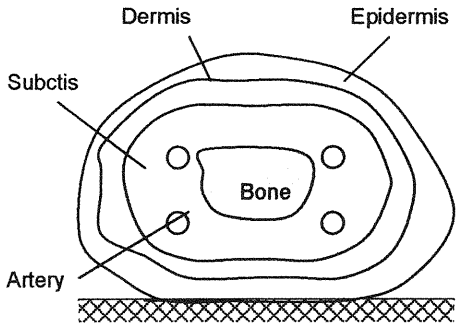

Fig. 2 Schematic of the cross-section of the human index finger.

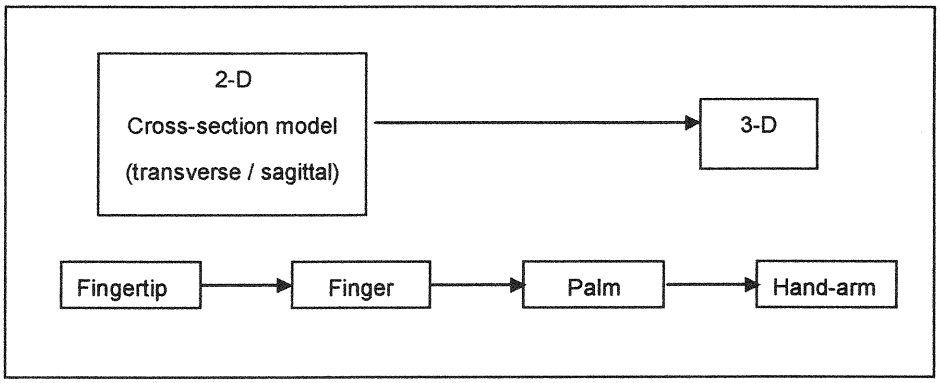

Fig. 3 Construction strategy of the FE hand-arm model

2.3 Heat Transfer in Bio-tissue

2.3.1 General Formulation

Heat transfer in bio-tissues is modeled in the following bioheat equation (Pennes 1948):

$$\rho c \frac{\partial T}{\partial t} = \nabla \cdot (k_t \nabla T) - \rho_b w_b c_b (T - T_a) + q_m \tag{1}$$

where T is the tissue temperature, T_a the temperature of the arterial blood, ρ the density of the tissue, ρ_b the density of the blood, c the volumetric specific heat of the tissue, c_b the specific heat of the blood, k_t the thermal conductivity of the tissue, w_b the blood perfusion rate per unit volume in tissues, q_m the metabolic heat generation rate per unit volume in tissues, respectively. The first and second terms in the right side of the equation denotes the isotropic generation of heat transferred by blood perfusion and the metabolic heat generation in the tissue, respectively. This formula assumes that the arterial blood flowing into blood vessels for heat exchange, instantly fall into a thermal equilibrium, changing its temperature from the initial temperature T_a to the tissue temperature T.

2.3.2 Boundary Condition

The thermal boundary condition at the surface of finger skins is given as follows:

$$k_t \frac{\partial T}{\partial n} = h_{ca}(T - T_m) + h_{ra}(T - T_m) + E_{sk} \quad (2)$$

where h_{ca} denotes the convection heat transfer coefficient between the skin and the ambient air, h_{ra} the radiation heat transfer coefficient between the skin and the ambient air, E_{sk} the evaporative heat loss, T_m the ambient temperature, respectively. The flow velocity in ambient air influences the heat transfer behavior between the ambient air and the surface of fingers. When the ambient airflow velocity V is in the range of $0<V<0.15$ (m/s), on the assumption of an indoor situation, h_{ca} and h_{ra} can be regarded as invariant, 3.9 (W/m^{2}K) and 4.7 (W/m^{2}K), respectively.

The evaporative heat loss E_{sk} from the skin surface can be estimated in the following equation:

$$E_{sk} = h_e \cdot (P_s - P_m) \quad (3)$$

where h_e is the evaporative coefficient, empirically given as a function of the ambient airflow velocity V:

$$h_e = 124\sqrt{V} \quad (4)$$

P_s and P_m denote the saturated water vapor pressure at the skin surface temperature and that at the ambient temperature, respectively.

In contrast, the thermal boundary condition corresponding to the heat transfer between arteries and finger tissues is given as follows:

$$k_t \frac{\partial T}{\partial n} = h_a(T - T_a) \quad (5)$$

where h_a denotes the convection heat transfer coefficient between the artery blood and the finger subctis tissue, the value of which is 1,800 (W/m^{2}K).

2.3.3 Modeling of Vibration-induced Vasoconstriction

Vasoconstriction has been reported to occur in digits exposed to HTV.This vasoconstriction yields a decrease in skin temperature in vibration-exposed fingers. (Kondo, Sakakibara et al. 1987) This is because the blood perfusion rate of tissues in digits exposed to HTV decreases as a result of vasoconstriction induced by vibration, resulting in a decrease in heat supply to the digit tissue with blood perfusion. In this study we mathematically model the blood perfusion rate per unit volume in tissues w_b, based on experimental data reported in a previous study, as follows:

$$w_b(t) = \begin{cases} w_0 & (t < t_1) \\ cw_0 + (1-c)w_0 \exp\left[-\dfrac{t}{\tau_1}\right] & (t_1 \le t \le t_2) \\ w_0 - \{w_0 - w_b(t_1)\}\exp\left[-\dfrac{t}{\tau_2}\right] & (t_2 < t) \end{cases} \quad (6)$$

where **c** is a constant given a value between 0 and 1, denoting the minimum blood perfusion rate

observed at time t_2 as $\boldsymbol{cw_0}$. w_0 is the base blood perfusion rate. t_1 and t_2 are the time when vibratory application starts and stops, respectively. τ_1 and τ_2 are time constants characterizing the decreasing and recovery speed of the blood perfusion rate during and after vibration, empirically given based on experimental data, respectively .

The base blood perfusion rates per unit volume in tissues comprising the hand-arm system are shown in Table 2 with other physical properties of tissues required in eq. (1).

Table 2. Physical properties and blood perfusion rate of tissues.

	Bone	Subctis	Dermis	Epidermis	Blood
ρ(kg/m^3)	1418	1270	1200	1200	1100
C (J/kgK)	2094	3768	3391	3391	3300
k_t (W/mK)	2.21	0.35	0.53	0.21	0.50
w_0 (ml/ml/min)	2.0/100	3.43/100	24/100	0	-

2.4 Wave Propagation Analysis

2.4.1 General Formulation

Dynamic response of bio-tissues is subjected to a wave propagation phenomenon in viscoelastic materials, which suggests the loss of vibration energy characterized by vibratory attenuation. Thus the wave equation in the bio-tissue is given as follows:

$$\rho\frac{\partial^2 u}{\partial t^2}+\mu\frac{\partial u}{\partial t}+\nabla(K\nabla\cdot u)=f(t) \tag{7}$$

where ρ is the density, μ the attenuation coefficient, K the bulk modulus of the bio-tissue, respectively. $\boldsymbol{f}$ is the exterior force vector and $\boldsymbol{u}$ the displacement vector at a certain position at time t, respectively. In this study the exterior force vector is represented by the summation of the reaction force vector $\boldsymbol{F}$ to a static push force vector and the dynamic inertia force $-\rho\cdot a(t)$, applied to a surface of the tissue.

$$f(t)=F-\rho\cdot a(t) \tag{8}$$

where a(t) is the forced acceleration.

2.4.2 Modeling of Mechanical Properties

Human hand-arm system consists of several distinct layers and components of tissues. Hence the hand-arm system exhibits complex material behavior. For simplification, we take an example of human fingertips. Fingertips consist of several components, nail, epidermis, dermis, subctis, bone, and blood vessels, among which only nail and bone can be regarded as elastic or rigid in a certain loading condition. The other tissues comprising fingertips are classified into soft (hydrated) tissues, which generally behave as a non-homogeneous, anisotropic, non-linear viscoelastic material. In this study the viscoelastic properties of the soft tissues are described based on the biphasic theory. Non-homogeneity and anisotropic mechanical property of the soft tissues will be considered at the next step.

The mechanical properties of these tissues have been reported to be affected by temperature and

water content (humidity).(Wildnauer, Bothwell et al. 1971; Papir, Hsu et al. 1975) In order to obtain a better description of the mechanical behavior of finger tissues, the effects of the temperature and water content as well as the structure of the tissues must be taken into account. Although, these data includes those measured in rat skins and of human upper back skins, they can be available to understand the general relationship between the Young's modulus and these environmental parameters. We model the Young's modulus of the soft tissue in hand-arms as a function of the surface temperature and the water content (the relative humidity):

$$E = E(T,H) = E_1 + E_0(T)\cdot \exp\left[-\frac{H}{H_\tau}\right] \tag{9}$$

where T denotes the tissue temperature and H the relative humidity of the tissue. E_1 and E_0 denotes the young's modulus of the tissue at a relative humidity of 0%, and that at a relative humidity of 100%, respectively. H_τ is a constant obtained from experiments. An experimental study on measurement of Young's moduli of skin tissues using a small indentation probe has reported that the young's modulus of epidermis was proportional to those of dermis and subctis in human finger tissues, given as the following relationship. (Maeno et al. 1998)

$$E_{epidermis} : E_{dermis} : E_{subctis} \cong 8:5:2$$

In this study we incorporate this relationship into our mechanical property model.

2.5 Discretization with the Galerkin Method

2.5.1 Discretization of Heat Transfer Equation

Substituting a finite element approximation for T into the weak form of the weighted residual heat transfer equation of bio-tissues yields the semidescrete finite element model, given as

$$\begin{aligned}&\rho c[M_T]\{\dot{T}\}^{(n)} + [k_t[k_x] + k_t[k_y] + \rho_b w_b c_b[M]]\{T\}^{(n)} \\ &\quad = \rho_b w_b c_b T_b[L] + q_m[L] + (h_{ca} + h_{ra} + h_a)[f_\Gamma]\{T\}^{(n)} + (E_{sk} - (h_{ca} + h_{ra} + h_a)T_m)[g_\Gamma]\end{aligned} \tag{10}$$

where a superposed dot on T denotes a derivative with time. The blood perfusion rates per unit volume in tissues w_b are updated at every computation step using eq. (6). The element coefficient matrices appear in eq. (10) are written in the following forms:

$$[M_T] = \int_{\Omega_e}{}^T N\cdot N d\Omega, \quad [k_x] = \int_{\Omega_e}{}^T N_x N_x d\Omega, \quad [k_y] = \int_{\Omega_e}{}^T N_y N_y d\Omega, \quad [L] = \int_{\Omega_e} N d\Omega \tag{11}$$

$$[f_\Gamma] = \int_\Gamma{}^T N\cdot N d\Gamma, \quad [g_\Gamma] = \int_\Gamma N d\Gamma \tag{12}$$

where N denotes the interpolation function for finite elements and subscripts x and y denote the partial differentiation on x and y, respectively.

Temperature distributions at arbitrary time t can be obtained by integrating eq. (10) in time domain. Application of a well-known integration method of Runge-Kutta scheme to time integration in eq. (10) yields the solution vector of temperatures with fourth order accuracy, given as follows:

$$\{T\}^{(n+1)} = \{T\}^{(n)} + \frac{1}{6}(C_0 + 2C_1 + 2C_2 + C_3) \tag{13}$$

$$C_0 = \Delta t \cdot \left([P]\{T\}^{(n)} + \{Q\}^{(n)}\right), \qquad C_1 = \Delta t \cdot \left[[P]\left(\{T\}^{(n)} + \frac{1}{2}C_0\right) + \{Q\}^{(n+\frac{1}{2})}\right]$$

$$C_2 = \Delta t \cdot \left[[P]\left(\{T\}^{(n)} + \frac{1}{2}C_1\right) + \{Q\}^{(n+\frac{1}{2})}\right], \quad C_3 = \Delta t \cdot \left[[P]\left(\{T\}^{(n)} + C_2\right) + \{Q\}^{(n-1)}\right] \tag{14}$$

$$[P] = \frac{1}{\rho c}[M_T]^{-1}\left[-k_t[k_x] - k_t[k_y] - \rho_b w_b c_b[M] + (h_{ca} + h_{ra} + h_a)[f_\Gamma]\right] \cdot \{T\}^{(n)} \tag{15}$$

$$\{Q\}^{(n)} = \frac{1}{\rho c}\left[\ \rho_b w_b c_b T_b[L] + q_m[L] + \left(E_{sk} - (h_{ca} + h_{ra} + h_a)T_m\right)[g_\Gamma]\ \right] \tag{16}$$

2.5.2 Discretization of Momentum Equation

In this study the vibration response of bio-tissues is modeled as a linear dynamic response problem with attenuation, given as follows:

$$[M_V]\{\ddot{u}\}^{(n)} + [C]\{\dot{u}\}^{(n)} + [K]\{u\}^{(n)} = \{f\}^{(n)} \tag{17}$$

where the element coefficient matrices appear in eq. (17) are written in the following forms:

$$[M_V] = \int_{\Omega_e} N^T \rho N d\Omega, \quad [C] = \int_{\Omega_e} N^T \mu N d\Omega, \quad [K] = \int_{\Omega_e} B^T D B d\Omega \tag{18}$$

Application of Euler central difference scheme yields the velocity and acceleration vectors at time t given in the following equations:

$$\{\dot{u}\}^{(n)} = \frac{1}{2\Delta t}\left(\{u\}^{(n+1)} - \{u\}^{(n-1)}\right) \tag{19}$$

$$\{\ddot{u}\}^{(n)} = \frac{1}{\Delta t^2}\left(\{u\}^{(n+1)} - 2\{u\}^{(n)} + \{u\}^{(n-1)}\right) \tag{20}$$

Substituting eqs. (18) and (19) into eq. (16) yields the following equation:

$$\{u\}^{(n)} = \left[[M_V] + \frac{\Delta t}{2}[C]\right]^{-1}\left\{\Delta t^2\left[\{f\}^{(n)} - [K]\{u\}^{(n)}\right] + 2[M_V]\{u\}^{(n)} - \left[[M_V] - \frac{\Delta t}{2}[C]\right]\{u\}^{(n-1)}\right\} \tag{21}$$

The velocity and acceleration vectors at time t obtained by substituting eq.(21) into eqs. (19) and (20), can be used to evaluate dynamic responses of the living soft tissue in the hand-arm system.

3. Current Status

A simple simulation was performed to evaluate the validation of the vibration-induced vasoconstriction model. In this simulation, application of vibration started at 120 (sec) and stopped at 240 (sec). Figure 4 shows the blood perfusion rate curves of dermis in the tissue. The environmental temperature was fixed to 22.0℃.The initial skin and internal tissue temperature was set to 32.0℃. Figure 5 shows the change of the skin temperature obtained from the simulation. The result showed good agreement to experimental data reported in a previous study. (Kondo et al. 1987)

In the next step, we plan to perform coupling of the heat transfer equation with the wave propagation equation, where the mechanical properties of the finger tissues modeled as a function of temperature

and water content will be incorporated.

4. Conclusion

This paper introduced the development of a computational hand-arm system that can predict the dynamic responses of the hand-arm system exposed to HTV under arbitrary environmental conditions characterized by environmental temperature, humidity, surface temperature of tool grips, perspiration in palms, and so on. As the first report of this study, this paper stressed the general concept of fabrication of a novel biodynamic response model based on FEM in the computational hand-arm system that couples the heat transfer equation in bio-tissues with the wave propagation equation. Also we addressed to modeling of vasoconstriction in hand-arms exposed to HTV and that of the tissue mechanical properties dependent on thermal environment and moisture.

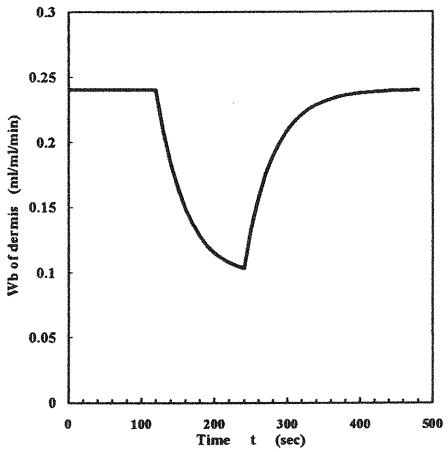

Fig. 4 The blood perfusion rate change of dermis vibration-induced induced vasoconstriction.

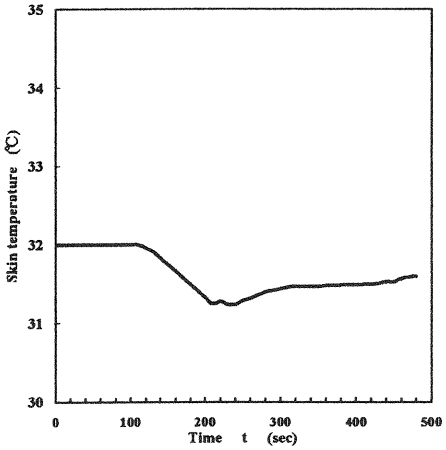

Fig. 5 The change of skin temperature..

5. Reference

M.Bovenzi (1998). "Exposure-response relationship in the hand-arm vibration syndrome: an overview of current epidemiology research." International Archives of Occupational and Environmental Health **71**(8): 509-519.

K. Dandekar, B. I. Raju, et al. (2003). "3-D Finite-element models of human and monkey fingertips to investigate the mechanics of tactile sense." Journal of Biomechanical Engineering. **125**: 682-691.

R. G. Dong, S. Rakheja, et al. (2001). "Hand-transmitted vibration and biodynamic response of the human hand-arm: a critical review." Critical Reviews in Biomedical Engineering **29**(4): 393-439.

R. G. Dong, J. Z. Wu, et al. (2005). "Recent advances in biodynamics of human hand-arm system." Industrial Health **43**(3): 449-71.

H. Gray and C. D. Clemente (1985). Anatomy of the human body., Lea & Febiger, UK.

T. Kondo, H. Sakakibara, et al. (1987). "Effect of eposure to Hand-transmitted vibration on digital skin temperature change." Industrial Health **25**: 41-53.

T. Maeno, K. Kobayashi, et al. (1998). "Relationship between the structure of human finger tissue and the location of tactile receptors." JSME International Journal. **41**: 94-100.

N. J. Mansfield (2004). Human response to vibration. Boca Raton, CRC Press.

V. C. Mow, S. C. Kuei, et al. (1980). "Biphasic creep and stress relaxation of articular cartilage: theory and experiment." Journal of Biomechanical Engineering. **102**: 73-84.

Y. S. Papir, K. H. Hsu, et al. (1975). "The mechanical properties of stratum corneum I. the effect of water and ambient temperature on the tensile properties of newborn rat stratum corneum." Biochimica et Biophysica Acta **399**: 170-180.

P. L. Pelmear and D. Leong (2000). "Review of occupational standards and guidelines for hand-arm (segmental) vibration syndrome (HAVS)." Applied Occupational and Environmental Hygiene **15**(3): 291-302.

H. H. Pennes (1948). "Analysis of tissue and arterial blood temperatures in the resting human forearm." Journal of Applied Physiology **1**(2): 93-122.

M. Srinivasan and K. Dandekar (1996). "An investigation of the mechanics of tavtile sense using two-dimensional models of the primate fingertip." Journal of Biomechanical Engineering. **118**: 48-55.

R. H. Wildnauer, J. W. Bothwell, et al. (1971). "Stratum corneum biomechanical properties I. influence of relative humidity on normal and extracted human stratum corneum." The Journal of Investigative Dermatology **56**(1): 72-78.

J. Z. Wu, R. G. Dong, et al. (2002a). "Simulation of mechanical responses of fingertip to dynamic loading." Medical Engineering and Physics. **24**(4): 253-64.

J. Z. Wu, S. Rakheja, et al. (2002b). "Effects of static compression on the vibration modes of a fingertip." Journal of Low Frequency Noise, Vibration and Active Control **21**(4): 29-243.

COMPARISON OF HUMAN VIBRATION MEASUREMENT BY A LASER DOPPLER VIBROMETER AND AN ACCELEROMETER

Setsuo Maeda
Hazard Evaluation and Epidemiology Research Group
Japan National Institute of Occupational Safety and Health
(JNIOSH)
21-1, Nagao 6-Chome, Tama-ku
Kawasaki 214-8585
Japan
E-Mail: maedas@h.jniosh.go.jp

Masakazu Ozaki
Brüel & Kjær division of Spectris Co.Ltd., Japan,
3−5−24 Miyahara Yodogawa
Osaka 532-0003
Japan
E-Mail : mozaki@bksv.com

Abstract

The purpose of this paper is to demonstrate the two different kinds of the human vibration measurement equipments and the comparison of human vibration measurement by a Laser Doppler Vibrometer and an Accelerometer. The handle vibration was measured by an accelerometer which mounted on a handle attached a vibrator and by a Laser Doppler Vibrometer. From the comparison of the measurement results of two equipments, the advantages and disadvantages of this measurement technique is demonstrated in this paper.

Introduction

There are many instruments to measure the human vibration in the world. These devices mean Whole-Body Vibration Meter, Hand-Arm Transmitted Vibration Meter. These equipments consist of all-in-one type or computer based equipments.

Presented at the 14th Japan Conference on Human Responses to Vibration,
Held in T.M.U., Hachioji, Tokyo, Japan, Aug 2nd to 4th, 2006.

There are many instruments to measure the vibration. Figure 1 shows the examples of these instruments.

Figure 1. Examples of measurement instruments of vibration.

These instruments as shown in Figure 1 can measure the whole-body and the hand-arm vibration in the laboratory and in the field. These measurement equipments are using the accelerometer to measure the vibration. On the measurement, the accelerometer has to mount on the materials or the

devices or the handles of the tools or the resilient materials. In these measurements, the problem of the weight of accelerometer has been demonstrated (Maeda, 2000). Also, the problem of the attached resonance of the accelerometer has been reported (Hayashi et al, 2005). Therefore, the method or the equipment needs to measure the vibration to eliminate the problems of accelerometer measurement. Although the Laser Vibrometer Measurement has been proposed by researchers (Beboli et al, 1999), they did not show the exact results in their paper. So, from their results, the advantages and disadvantages couldn't get.

Therefore, in this paper, the handle vibration was measured by an accelerometer which mounted on a handle attached a vibrator and by a Laser Doppler Vibrometer. The two different kinds of the human vibration measurement equipments and the comparison of human vibration measurement by a Laser Doppler Vibrometer and an Accelerometer were demonstrated.

Experiment

Apparatus

The measurement apparatus of this experiment is shown in Figure 1 and Figure 2.

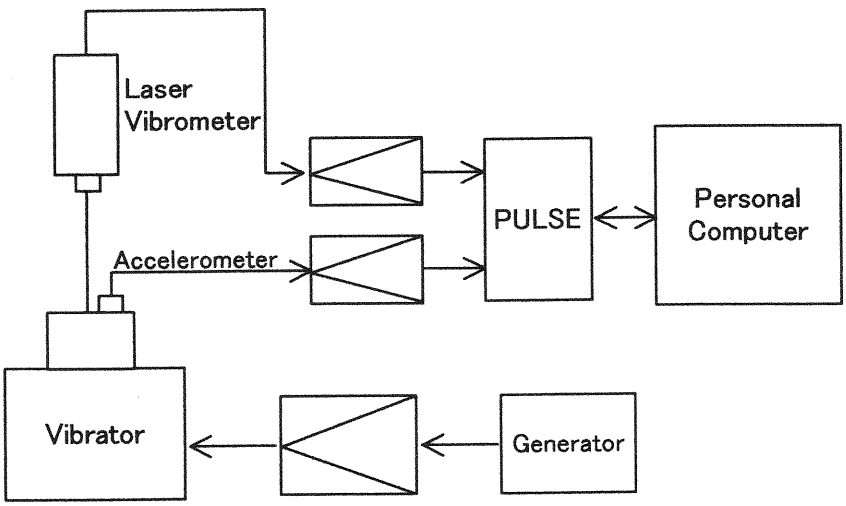

Figure 1. Measurement apparatus of a Laser Doppler Vibrometer and an Accelerometer.

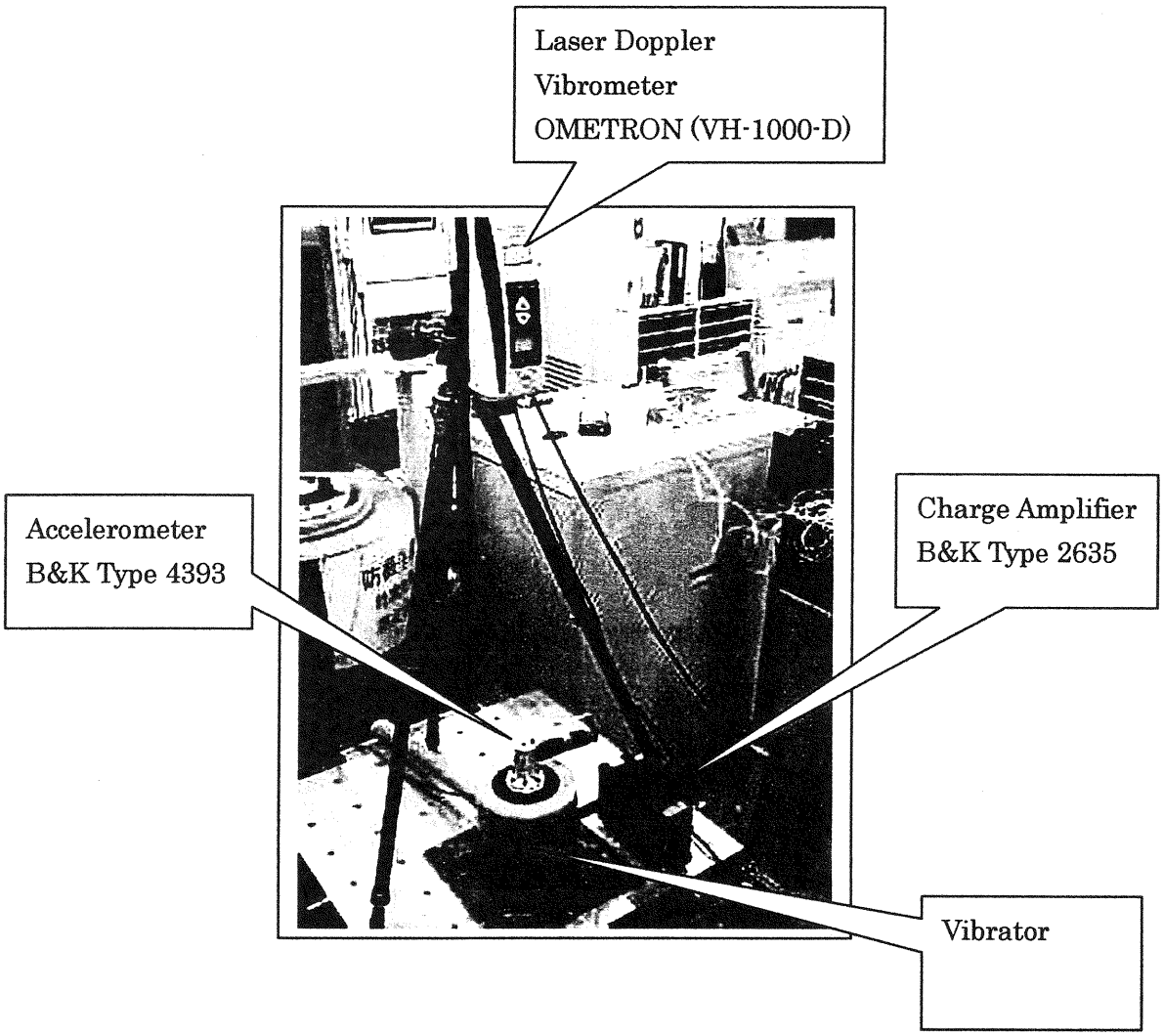

Figure 2. Experimental set-up in this experiment.

Measurement of physical parameters

The following physical quantities were measured in this experiment.

1) Rms of handle vibration in Z axis with a Laser Doppler Vibrometer.

2) Rms of handle vibration in Z axis with piezoelectric accelerometer mounted on the handle.

The vibration data from two equipments were acquired by a PULSE-X system. After getting vibration data, the 1/3 octave band analysis was performed by PULSE software. And LDV data were compared with the piezoelectric accelerometer.

The optimal stand-off distance from the mounting surface of the front panel of LDV is calculating by the following equation:

$$X = 100\ mm + n \cdot 138\ mm$$

$$n = 0, 1, 2, 3, 4, 5, 6, 7, 8, 10, \cdot \cdot \cdot$$

The light source of the VH-1000-D is a helium neon laser. The visibility maximum is present once per laser cavity length. In practice, it is not usually necessary to search for the visibility maximum , as the VH-1000-D is sensitive enough to make a measurement even close to the maximum. Table 1 and Table 2 show the characteristics of a Laser Doppler Vibrometer of the VH-1000-D. From these table, the LDV measurement does not think about the resonance of the vibration measurement like the accelerometer measurement and also the mounting method.

Table 1 Measurement Ranges of Laser Doppler Vibrometer of VH-1000-D (OMETRON)

Measurement range, full scale (peak) mm/s	Maximum acceleration m/s^2
20	2760
100	13800
500	69000

Table 2 Low pass filter.

Filter setting	Stop band
1 KHz	> 4.3 KHz
5 KHz	> 8.4 KHz
22 KHz	> 25 KHz

Results

Figure 3 shows the result of two equipments. This figure shows the result of vibration calibrator of B&K Type 4292.

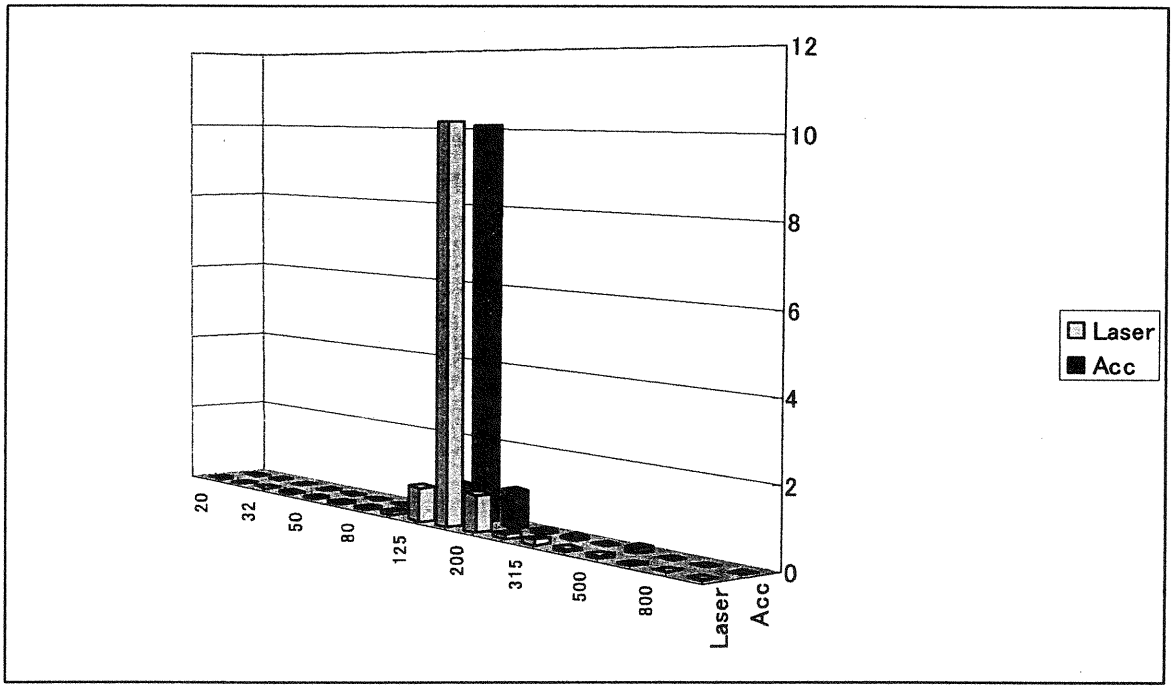

Figure 3. Comparison result of a LDV and an Accelerometer by using the vibration calibrator of B&K Type 4292.

From this figure, it was clear that the results from two equipments are the same. And, the pink noise vibration was generated by the vibrator handle and measured by LDV and Accelerometer.

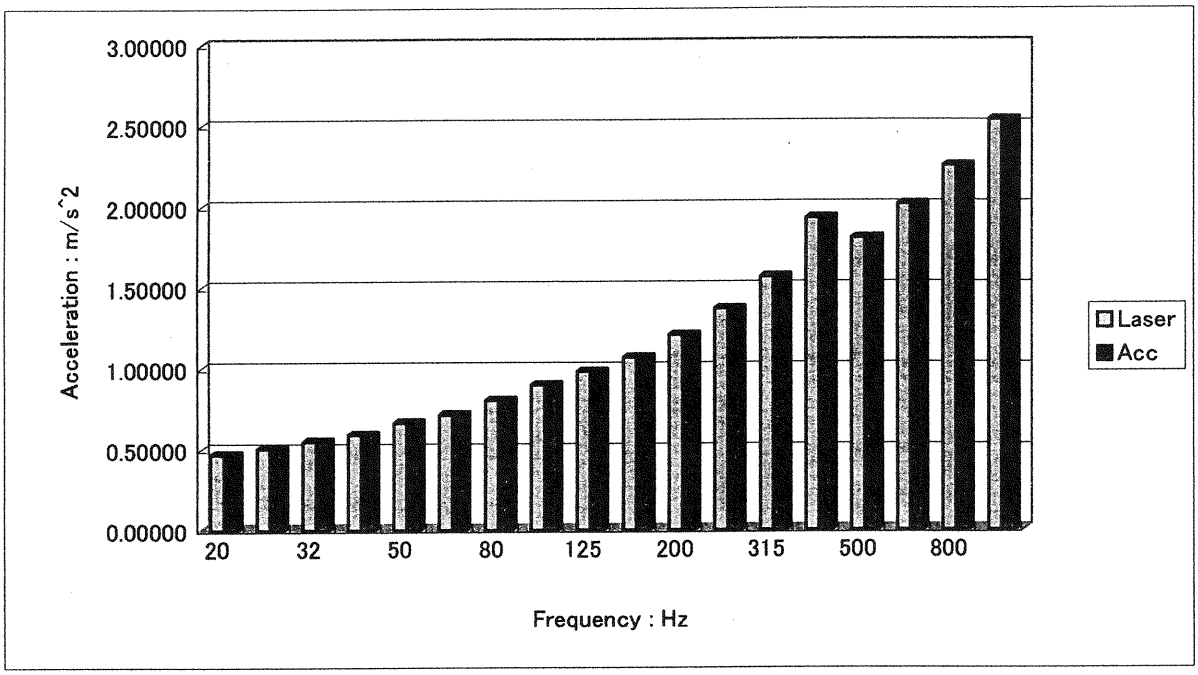

Figure 4. Comparison results of Vibration of two equipments.

From this trial measurement using two equipments, especially, on the measurement of a Laser Doppler Vibrometer, it was clear the advantage and the disadvantage of two vibration measurement equipments as shown in Table 3.

Table 3. Comparison of advantage and disadvantage of two measurement equipments.

	Laser Doppler Vibrometer	Accelerometer Measurement
Advantage	Easy measurement Don't need to think about 1: mounting method 2: resonance of transducer 3: resonance of mounting	
Disadvantage		Mounting method Resonance of transducer Resonance of mounting

Conclusions

In this paper, the comparison of human vibration measurement by a Laser Doppler Vibrometer and an Accelerometer were demonstrated. And also, the advantages and disadvantages of two vibration measurement equipments were cleared.

References

Beboli R, Paone N, Rossi GL (1999) Comparison of laser vibrometers and accelerometers to measure hand arm transmitted vibration, Proceedings of the 34th United Kingdom Group Meeting on Human Response to Vibration, Ford Motor Company, Dunton, Essex, England, 22-24 September 1999.

Hayashi K, Mizuno S, Sano Y, Naruse H (2005) Measurements and investigations of vibration on the tatami mat. – Examination about vertical contact resonance of the vibration pickup by a measurement condition, The document of Noise and Vibration Research Meeting of JASJ, N-2006-28, 1-7.

Maeda S (2000) Effect of mass loading on the vibration measurement value of hand-held tools, Proceedings of CAIRNS 2000, 36.

日本産業衛生学会東海地方会
第２０回振動障害研究会

手持動力工具振動値のラベリング方法について

前田節雄
有害性評価研究グループ
労働安全衛生総合研究所
maedas@h. jniosh. go. jp

Brief introduction about JNIOSH

National Institute of Industrial Safety
産業安全研究所

+

National Institute of Industrial Health
産業医学総合研究所

=

National Institute of Occupational Safety
and Health, Japan (JNIOSH)
労働安全衛生総合研究所
From 1st April 2006

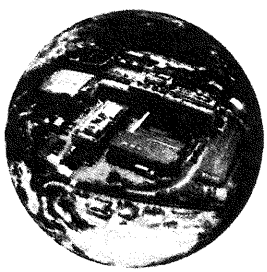

組織図

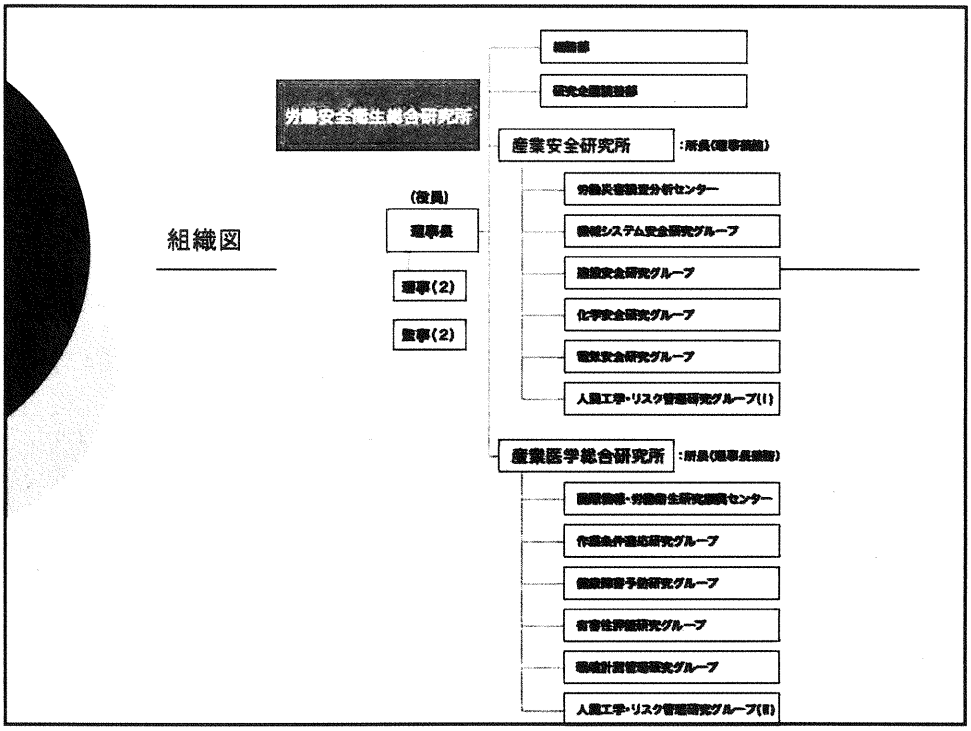

Japan National Institute of Occupational Safety and Health
Institute of Industrial Health

神奈川県川崎市多摩区長尾6－21－1

Home Page:
http://www.jniosh.go.jp/

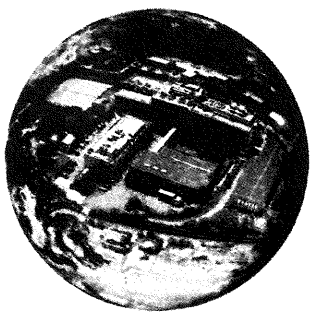

Hand-Arm Vibration

Vibration tools

↓

Prolonged vibration exposure

↓

Vibration syndrome

Raynaud's phenomenon

Vibration white finger (VWF)

Vibration syndrome

Hand-Arm Vibration Syndrome